

# Probing Flow Velocity with Silicon Nanowire Sensors

Dong Rip Kim, Chi Hwan Lee, and Xiaolin Zheng\*

*Department of Mechanical Engineering, Stanford University, California 94305*

*Received January 22, 2009; Revised Manuscript Received March 5, 2009*

## ABSTRACT

We report our experimental efforts to quantify the impact of fluidic and ionic transport on the conductance level of silicon nanowire (SiNW) sensors configured as field effect transistors (FETs). Specifically, the conductance of SiNW FETs placed in a microfluidic channel was observed to change linearly with the flow velocity of electrolytic solutions. The direction of conductance change depends on the doping type of the SiNWs and their location inside the microfluidic channel, and the magnitude of the conductance change varies with the ionic strength and compositions of the electrolytic solution. Our quantitative analysis suggests that the flow velocity sensing is a consequence of the streaming potential that is generated by the movement of counterions inside the electrical double layer (EDL) of the silica substrate. The streaming potential, which varies with the flow velocity and the ionic properties of the electrolytic solution, acts in the same way as the charged analytes in affecting the conductance of SiNWs by changing the surface potential. This study highlights the importance of considering the ionic transport in analyzing and optimizing nanowire FET sensors, which can significantly change the conductance of NWs. Moreover, SiNWs were demonstrated for the first time to be able to detect the streaming potential, the flow velocity and the ionic strength, opening up their new application potentials in microfluidics.

Semiconducting NWs configured as FETs have recently attracted considerable attention because of their great potential as label-free, real-time, and ultrasensitive biological and chemical sensors.<sup>1-7</sup> In particular, SiNWs were successfully demonstrated to possess great selectivity in detecting a wide range of charged species, such as proteins, viruses, and DNAs.<sup>1-7</sup> The NW sensors typically operate in an electrolytic solution and respond to changes in the local electric potential caused by the specific binding and unbinding events between the receptors and the target molecules.<sup>8</sup> However, in the sensing environment, the charged analytes coexist with charged ions of the electrolytic solution and the variation in the ionic distribution in the vicinity of the NW sensors can also affect the local electric potential around the NWs. This will lead to a conductance change of the NWs, which may overshadow the signals from the specific binding events and impact the selectivity of NW FET sensors. The effects of the ionic distribution on the electric potential inside an aqueous solution have been recognized and utilized as the detection mechanism for the ion-sensitive field effect transistor (ISFET). Nonetheless, the electric properties of ions have frequently been neglected for simplicity when analyzing NW FET sensors by assuming the electrolytic solution to be charge neutral.<sup>9-11</sup> Therefore, it is important to investigate the impact of charged ions on the conductance level of NW FET sensors so that the performance of NW sensors can be further improved.

To understand the physics underlying the influence of ions on NW FET sensors, we have undertaken and report herein experimental efforts to quantify the impact of ions on the conductance level of SiNW FET sensors. Our experimental results indicate that the ionic distribution and the transport of the electrolytic solution can significantly affect the conductance level of SiNW FET sensors and that the interaction mechanism is closely related to the streaming potential generated by the streamwise ionic movement. Moreover, the effects of ions on SiNWs can be utilized to develop SiNW sensors to measure the flow velocity of the solution and to probe the properties of the solution.

The SiNWs were configured as FETs to detect flow velocity. The experimental setup is similar to previously reported SiNW FET sensing experiments,<sup>8</sup> as shown in Figure 1a, where SiNWs are located on the floor of the microfluidic channel. The channel consists of a Si/SiO<sub>2</sub> floor and a cover made from the polydimethylsiloxane (PDMS). Differently from some previous NW FET sensing experiments,<sup>8</sup> an Ag/AgCl reference electrode was placed in the center of the channel to fix the local electric potential of the solution and hence to reduce the noise generated by the drifting of the solution potential.<sup>12-14</sup> The SiNWs were synthesized using the vapor-liquid-solid mechanism with 20 nm gold nanoclusters, at a 4000:1 Si/B feeding ratio for the p-type and a 2000:1 Si/P feeding ratio for the n-type SiNWs, respectively.<sup>15-17</sup> Arrays of SiNW sensors were fabricated using photolithography with Ti/Pd as the source and drain metal contacts.<sup>8,18</sup> These contacts were further

\* Corresponding author. E-mail: xlzheng@stanford.edu.

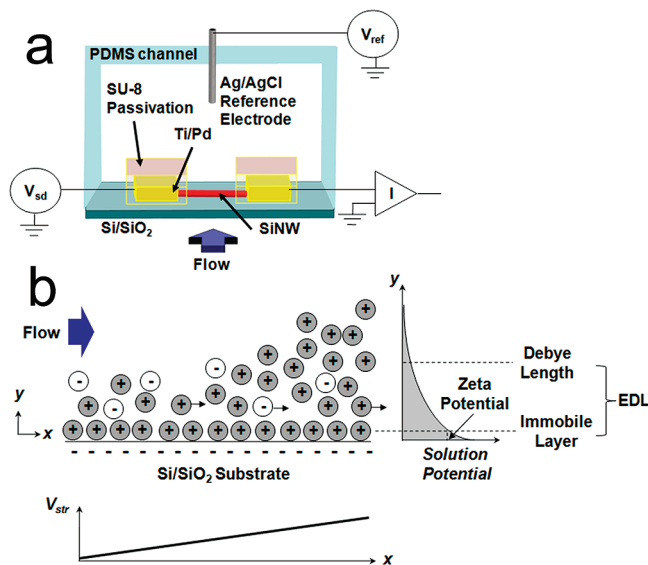


**Figure 1.** Experimental setup for the SiNW FET flow velocity measurement and its operating principle (not to scale). (a) Cross-section schematic of a SiNW sensor inside a microfluidic channel. (b) Operating principle of the SiNW FET flow velocity sensor: the excess counterions inside the EDL formed in the microfluidic channel are swept downstream by the pressure-driven flow, which generates the streaming potential ( $V_{str}$ ).

passivated with SU-8 to prevent the leakage of current into the electrolytic solution. The SU-8 passivation quality was excellent because devices did not exhibit any noticeable degradation over 1 week of sensing experiments. The conductance of SiNWs was measured using lock-in detection by applying a 30mV voltage with a frequency of a few kHz and measuring the current.<sup>8</sup> The electrolytic solutions used in this study were potassium chloride in potassium phosphate buffers, unless mentioned otherwise. The pH value of the solution was 7, achieved by mixing the monobasic ( $\text{KH}_2\text{PO}_4$ ) and dibasic ( $\text{K}_2\text{HPO}_4$ ) potassium phosphates in DI water. The ionic strength of the solution was controlled by diluting the solution with DI water and adding potassium chloride (KCl). The flow velocity of the solution inside the microfluidic channel was controlled by a syringe pump (Harvard Apparatus).

The interaction mechanism between the ions and the SiNWs is illustrated in Figure 1b. When the surface of the silica substrate and the SiNWs contacts liquid solutions with pH values greater than the isoelectric point of the silica ( $\sim 2-3$ ), the surface becomes negatively charged due to the deprotonation of the silanol groups [ $\text{SiOH}(s) \rightarrow \text{SiO}^-(s) + \text{H}^+(\text{aq})$ ]. The charged surface attracts a layer of counterions next to the silica surface to maintain the overall charge neutrality, forming an EDL. The distribution of ions inside the EDL affects the surface potential of the SiNWs and through which influence the conductance level of the SiNW FET sensor.<sup>12</sup> When the electrolytic solution is flowing, it carries the excess counterions (cations) in the mobile part of the EDL downstream. Charges are accumulated at both ends of the channel and a longitudinal electrical field is established across the channel (Figure 1b), which is the streaming potential ( $V_{str}$ ). The streaming potential has been

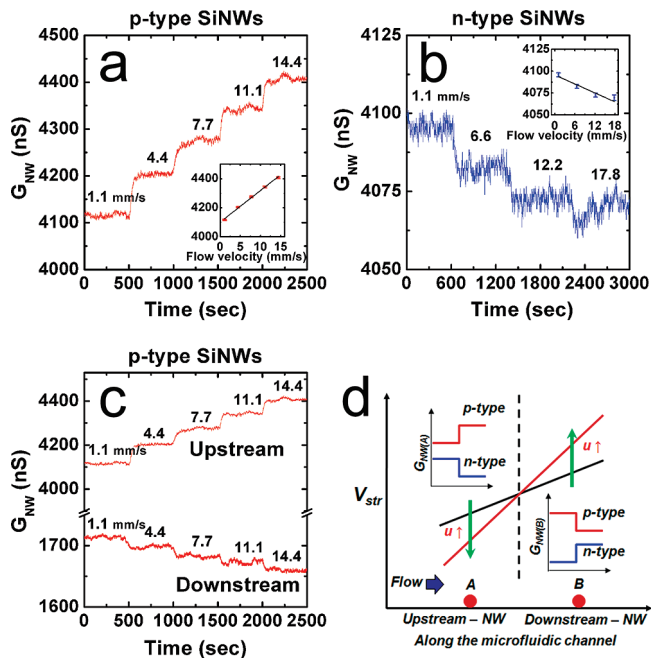


**Figure 2.** Flow velocity sensing using p-type and n-type SiNWs. (a) Conductance ( $G_{NW}$ ) of p-type SiNWs as a function of the flow velocity. (Inset)  $G_{NW}$  versus flow velocity. (b)  $G_{NW}$  of n-type SiNWs as a function of the flow velocity. (Inset):  $G_{NW}$  versus flow velocity. (c) Opposite trends of  $G_{NW}$  change in flow velocity sensing for differently located p-type SiNWs in the microfluidic channel. (d) Illustration of location-dependent  $G_{NW}$  change of SiNWs in terms of the flow velocity. (The electrolytic solution contained 1  $\mu\text{M}$  potassium chloride in 0.1  $\mu\text{M}$  potassium phosphate buffer with pH 7 and its measured electrical conductivity ( $\sigma$ ) was 11.2  $\mu\text{S cm}^{-1}$ .)

studied both theoretically and experimentally<sup>19-24</sup> and can be expressed as functions of the flow velocity and the fluid properties as shown in eq 1, assuming the existence of a fully dissociated, symmetric electrolytic solution with equal mobilities, a thin EDL, and a hydrodynamically fully developed flow.

$$\Delta V_{str} = \frac{\epsilon_r \epsilon_0 \zeta}{\sigma \eta} \Delta P \sim \frac{\epsilon_r \epsilon_0 \zeta}{\sigma} \Delta u \quad (1)$$

Here,  $V_{str}$  is the streaming potential (V),  $\epsilon_r$  is the relative permittivity of the electrolytic solution,  $\epsilon_0$  is the vacuum permittivity ( $\text{F m}^{-1}$ ),  $\zeta$  is the zeta potential of the EDL on the microfluidic channel surface (V),  $\sigma$  is the electrical conductivity of the bulk solution ( $\text{S m}^{-1}$ ),  $\eta$  is the dynamic viscosity of the solution ( $\text{Pa s}$ ),  $P$  is the pressure (Pa), and  $u$  is the flow velocity ( $\text{m s}^{-1}$ ). Consequently, when the flow velocity changes, it modifies the streaming potential, which affects the ionic distributions in the EDL around the SiNWs; as a result, the conductance of NWs changes with the flow velocity.

Our experimental results support the fact that the flow velocity can significantly affect the conductance of SiNW FETs. As shown in Figure 2a and 2b, the conductances of both the p-type and the n-type SiNWs ( $G_{NW}$ ) change linearly with increasing flow velocity. The direction of the conductance change is opposite for the p-type and the n-type SiNWs

**Table 1.** Estimation of the Equivalent Gate Potential Change Per Unit Flow Velocity Change

	unit	p-type SiNWs	n-type SiNWs
$\Delta G_{NW}/\Delta V_{G,NW}$	(nS mV <sup>-1</sup> )	5.60	0.45
$\Delta G_{NW}/\Delta u$	(nS s mm <sup>-1</sup> )	21.8	1.6
$\Delta V_{G,NW}/\Delta u$	(mV s mm <sup>-1</sup> )	3.9	3.6

because the same gate potential change has the opposite depletion/accumulation effects on the p- and n-type SiNWs, respectively. The minimum velocity change which can be detected by the p-type SiNW is in the range of 0.55–1.1 mm s<sup>-1</sup>, which is more than one order of magnitude better than the reported flow velocity sensitivity of 20.83 mm s<sup>-1</sup> using individual carbon nanotube FET sensors.<sup>25</sup> To the best of our knowledge, this is the first experimental demonstration that SiNW FET sensors can measure the flow velocity change through the streaming potential mechanism in an electrolytic solution.

We further estimated the equivalent gate potential change per unit flow velocity ( $\Delta V_{G,NW}/\Delta u$ ) for both the p-type and the n-type SiNWs to compare the gate voltage change caused by the streaming potential. Specifically, the equivalent gate potential change per unit flow velocity ( $\Delta V_{G,NW}/\Delta u$ ) was estimated using eq 2, by dividing the averaged SiNW conductance change per flow velocity change ( $\Delta G_{NW}/\Delta u$ ) by the transconductance of SiNWs measured in the same solution ( $\Delta G_{NW}/\Delta V_{G,NW}$ ). The results are listed in Table 1.

$$\frac{\Delta V_{G,NW}}{\Delta u} = \frac{\Delta G_{NW}/\Delta u}{\Delta G_{NW}/\Delta V_{G,NW}} = \frac{\Delta V_{str}}{\Delta u} \sim \frac{\epsilon_r \epsilon_0 \zeta}{\sigma} \quad (2)$$

The equivalent gate potential changes per unit flow velocity for the p-type and the n-type SiNWs were very similar, at 3.9 mV s mm<sup>-1</sup> and 3.6 mV s mm<sup>-1</sup>, respectively. It should be noted that the measured p- and n-type SiNWs were located at almost identical positions inside the microfluidic channel and with respect to the reference electrode. Therefore, the observed near-equality of the local surface potential change per unit flow velocity strongly suggests that SiNWs are responding to the streaming potential change caused by the fluidic motion of an electrolytic solution.

Furthermore, even SiNWs of the same doping type can exhibit opposite conductance changes in response to increasing flow velocity when the SiNWs are located upstream and downstream of the reference electrode, respectively (Figure 2c). Because the electrical potential of solution is fixed at the center of the channel by the reference electrode (Figure 2d), the solution potential at the downstream and upstream locations increases and decreases with increasing the flow velocity, respectively. Consequently, even the same type of SiNWs, depending upon their locations, can detect the opposite potential change and respond oppositely to the same flow velocity change. This observation implies that the ionic transport will have different effects on FET sensors at different locations inside the microfluidic channel. This is of concern in biosensing because if the local electric potential change caused by the ionic transport is greater than that generated by the specific analyte–receptor binding event, it

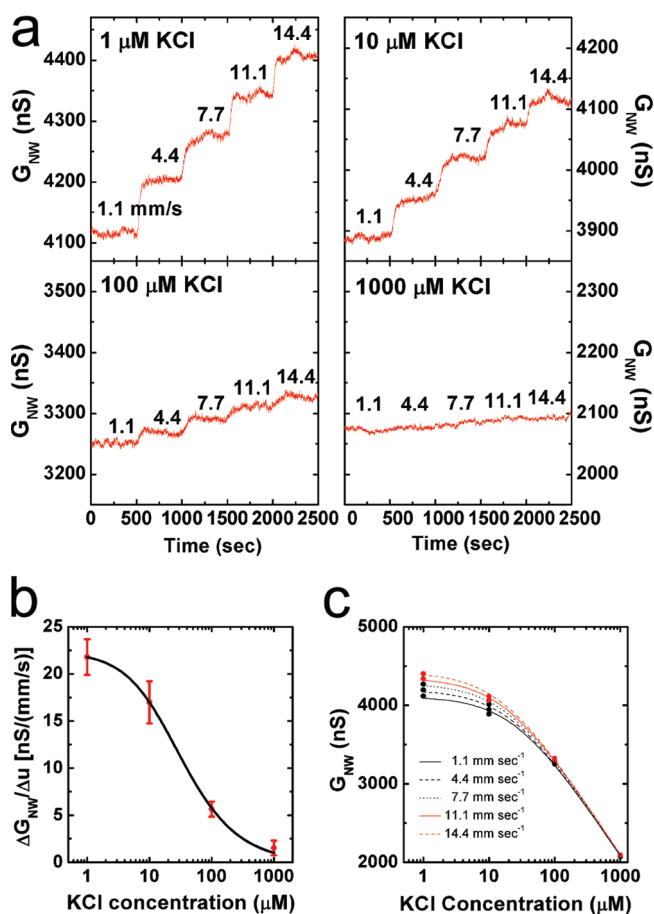


**Figure 3.** Effects of the ionic strength on the sensitivity of SiNW flow velocity sensing. (a) Flow velocity sensing of p-type SiNWs in potassium chloride solutions with ionic strengths of 1, 10, 100, and 1000  $\mu\text{M}$ . (b) The SiNW conductance change per unit flow velocity ( $\Delta G_{NW}/\Delta u$ ) with respect to the ionic strength (C). The solid line is a fitted curve,  $\Delta G_{NW}/\Delta u = (-162.5 + 391.8 \times \log(C + 10.9))/(C + 10.9)$ , where C is in  $\mu\text{M}$ . (c) The SiNW conductance ( $G_{NW}$ ) versus the ionic strength (C) at different flow velocities. All curves show logarithmic fittings:  $G_{NW} = 5887.0 - 1265.0 \times \log(C + 25.3)$  for  $u = 1.1 \text{ mm s}^{-1}$ ,  $G_{NW} = 5869.0 - 1258.0 \times \log(C + 21.3)$  for  $u = 4.4 \text{ mm s}^{-1}$ ,  $G_{NW} = 5901.0 - 1268.0 \times \log(C + 19.1)$  for  $u = 7.7 \text{ mm s}^{-1}$ ,  $G_{NW} = 5920.0 - 1271.0 \times \log(C + 17.2)$  for  $u = 11.1 \text{ mm s}^{-1}$ , and  $G_{NW} = 5944.0 - 1279.0 \times \log(C + 15.5)$  for  $u = 14.4 \text{ mm s}^{-1}$ , where C is in  $\mu\text{M}$ .

may produce false signals, such as an opposite conductance change.

The sensitivity of the flow velocity measurement for the p-type SiNW was further characterized as a function of the ionic strength of the electrolytic solution. The ionic strength of the potassium chloride solution (pH 7) was varied over a broad range, including strengths of 1, 10, 100, and 1000  $\mu\text{M}$ . As shown in Figure 3a, the conductance of the p-type SiNW ( $G_{NW}$ ) increases monotonically with increasing flow velocity for all the cases. However, the average amount of NW conductance change per unit flow velocity ( $\Delta G_{NW}/\Delta u$ ) decreases significantly as the ionic strength increases as shown in Figure 3b. The ionic strength affects the sensitivity of the flow velocity measurement by affecting both the solution conductivity ( $\sigma$ ) and the zeta potential ( $\zeta$ ) (eq 1). Specifically, the conductivity ( $\sigma$ ) of the solution is linearly proportional to its ionic strength,<sup>26,27</sup> and the zeta potential

( $\zeta$ ) has a logarithmic dependence on the ionic strength ( $\zeta \sim a_0 + a_1 \log C$ , where  $a_0$  and  $a_1$  are constants) for a symmetric electrolyte of  $C < 100$  mM at  $\text{pH} > 6$ .<sup>19</sup> The change of the streaming potential per unit flow velocity ( $\Delta V_{\text{str}}/\Delta u$ ), according to eq 1, is proportional to  $\zeta/\sigma$ , and varies with the ionic strength as  $(a_0 + a_1 \log C)/C$ . Furthermore, the SiNWs were selected to operate in the linear transconductance regime. Thus, the conductance change of the SiNWs ( $\Delta G_{\text{NW}}$ ) is linearly proportional to the change of the streaming potential ( $\Delta V_{\text{str}}$ ). Therefore, the conductance change of SiNWs per unit flow velocity ( $\Delta G_{\text{NW}}/\Delta u$ ) varies with the ionic strength as  $(a_0 + a_1 \log C)/C$ . Our experiments support this relation as shown in Figure 3b where the solid line is a fitted curve of  $\Delta G_{\text{NW}}/\Delta u = [-162.5 + 391.8 \times \log(C + 10.9)]/(C + 10.9)$  and 10.9 is a concentration correction term to account for the surface conductivity of the microfluidic channel.

Moreover, it can be seen from Figure 3c that the conductance levels of SiNWs ( $G_{\text{NW}}$ ) even at the same flow velocity are different for solutions with different ionic strengths and that  $G_{\text{NW}}$  decreases logarithmically with increasing ionic strength when the flow velocity and pH value are fixed. For example,  $G_{\text{NW}}$  can be related to the ionic strength through the logarithmic fitting of  $G_{\text{NW}} = 5887.0 - 1265.0 \times \log(C + 25.3)$  for  $u = 1.1 \text{ mm s}^{-1}$ , where 25.3 is, again, a correction to account for the surface conductivity. The similar dependence of the baseline conductance of NW FETs on the ionic strength of the solution was also observed for  $\text{SnO}_2$  nanobelt FET sensors in an aqueous solution.<sup>28</sup> The reason for this dependence is that the ionic strength affects the thickness of the EDL and the distribution of ions inside it. This changes the surface potential, through which the conductance of SiNWs is modified. The observation of the ionic strength-dependent conductance of SiNWs implies that SiNW FET sensors can potentially be utilized to measure the ionic strength of an electrolytic solution. As for NW biosensing, this observation indicates that the concentration of the analyte should be much smaller than the concentration of the buffer solution to prevent the conductance change of NWs induced by the change in the ionic strength of the buffer solution with/without the analyte.

The sensitivity of the flow velocity measurement also depends on the compositions of the electrolytic solutions since different solutions have different relative permittivity  $\epsilon_r$ , zeta potential  $\zeta$ , and electrical conductivity  $\sigma$  (eq 1). For the same n-type SiNW, the averaged conductance change in ethanol<sup>29</sup> was 3.8 times higher than that in a  $1 \mu\text{M}$  potassium chloride solution for the same flow velocity change, as shown in Figure 4a and 4b. This difference is consistent with the streaming potential difference estimated from their different properties according to eq 1 as shown in Table 2, where the estimated streaming potential change ( $\Delta V_{\text{str}}$ ) in ethanol is 3.2 times higher than that in  $1 \mu\text{M}$  potassium chloride, given the same flow velocity change. Hence, the larger conductance change of NWs ( $\Delta G_{\text{NW}}$ ) in ethanol comes from the larger streaming potential change generated in ethanol. Again, it suggests that SiNWs measure the flow velocity change by responding to changes in the

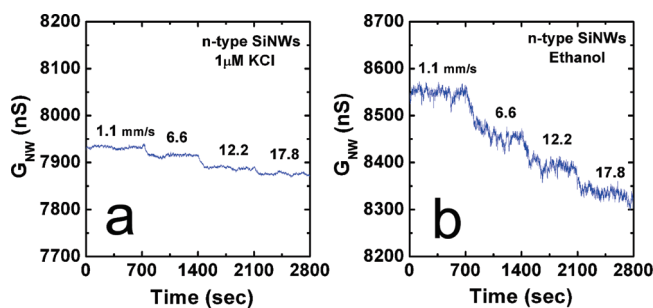


**Figure 4.** Effects of the ionic compositions on the sensitivity of SiNW flow velocity sensing. The conductance of SiNW ( $G_{\text{NW}}$ ) as a function of the flow velocity in (a) a  $1 \mu\text{M}$  potassium chloride solution and (b) an ethanol solution.

**Table 2.** Comparison of the Streaming Potential Generated by the  $1 \mu\text{M}$  Potassium Chloride Solution and Ethanol<sup>a</sup>

	unit	$1 \mu\text{M}$ potassium chloride	ethanol <sup>34</sup>
$\epsilon_r$		80.0	24.0
$\zeta$	(mV)	-100.0	-73.0
$\sigma$	( $\mu\text{S cm}^{-1}$ )	8.50	0.58
$\Delta V_{\text{str}} \sim \epsilon \zeta / \sigma$		1.0	3.2

<sup>a</sup> The relative permittivity and the zeta potential for the  $1 \mu\text{M}$  potassium chloride solution were assumed to be the same as the DI water because the solution was very dilute, and the electrical conductivity for both solutions was measured.

streaming potential. Furthermore, the observed enhanced sensitivity for measuring the flow velocity of ethanol indicates the versatility of the SiNW flow sensor and its potential to distinguish different solutions.

In summary, we have demonstrated the first flow velocity sensing of an electrolytic solution in a microfluidic channel using both the p-type and the n-type SiNW FET sensors. The conductance level of SiNWs reveals a clear and reproducible dependence on the flow velocity. The magnitude of conductance change of the SiNWs ( $\Delta G_{\text{NW}}$ ) depends on the ionic strength and the composition of the electrolytic solution, and the direction of  $\Delta G_{\text{NW}}$  depends on the doping type of the SiNWs and the location of the SiNWs in the microfluidic channel. Our quantitative analysis suggests that flow velocity sensing is a consequence of the streaming potential generated by the movement of counterions inside the EDL. The streaming potential, which varies with the flow velocity, the ionic strength and the composition of the electrolytic solution, acts in the same way as charged analytes in affecting the conductance of SiNWs. This study demonstrates that in addition to the analyte binding events, the properties and the velocity of the electrolytic solution can significantly change the conductance of NW FET sensors and it is important to consider these factors in analyzing and optimizing the sensing. Moreover, our study opens up a new type of sensing application for NW sensors in probing the streaming potentials, the flow velocity, the ionic strength, and more.

**Acknowledgment.** D.R.K. acknowledges support from the Link Foundation Energy Fellowship. X.L.Z. sincerely thanks the Center of Integrated System at Stanford University and the DARPA/YFA program for support of this work.

## References

- (1) Schoch, R. B.; Han, J. Y.; Renaud, P. *Rev. Mod. Phys.* **2008**, *80* (3), 839–883.
- (2) Cui, Y.; Wei, Q. Q.; Park, H. K.; Lieber, C. M. *Science* **2001**, *293* (5533), 1289–1292.
- (3) Hahm, J.; Lieber, C. M. *Nano Lett.* **2004**, *4* (1), 51–54.
- (4) Patolsky, F.; Zheng, G. F.; Hayden, O.; Lakadamyali, M.; Zhuang, X. W.; Lieber, C. M. *Proc. Natl. Acad. Sci. U.S.A.* **2004**, *101* (39), 14017–14022.
- (5) Patolsky, F.; Zheng, G.; Lieber, C. M. *Nanomedicine* **2006**, *1* (1), 51–65.
- (6) Patolsky, F.; Lieber, C. M. *Mater. Today* **2005**, *8* (5), 20–28.
- (7) Stern, E.; Klemic, J. F.; Routenberg, D. A.; Wyrembak, P. N.; Turner-Evans, D. B.; Hamilton, A. D.; LaVan, D. A.; Fahmy, T. M.; Reed, M. A. *Nature* **2007**, *445* (7127), 519–522.
- (8) Patolsky, F.; Zheng, G. F.; Lieber, C. M. *Nat. Protoc.* **2006**, *1* (4), 1711–1724.
- (9) Nair, P. R.; Alam, M. A. *Appl. Phys. Lett.* **2006**, *88* (23), 233120.
- (10) Squires, T. M.; Messinger, R. J.; Manalis, S. R. *Nat. Biotechnol.* **2008**, *26* (4), 417–426.
- (11) Kim, D. R.; Zheng, X. L. *Nano Lett.* **2008**, *8* (10), 3233–3237.
- (12) Shinwari, M. W.; Deen, M. J.; Landheer, D. *Microelectron. Reliab.* **2007**, *47* (12), 2025–2057.
- (13) Minot, E. D.; Janssens, A. M.; Heller, I.; Heering, H. A.; Dekker, C.; Lemay, S. G. *Appl. Phys. Lett.* **2007**, *91* (9), 093507.
- (14) Polk, B. J.; Stelzenmuller, A.; Mijares, G.; MacCrehan, W.; Gaitan, M. *Sens. Actuators, B* **2006**, *114* (1), 239–247.
- (15) Wagner, R. S.; Ellis, W. C. *Appl. Phys. Lett.* **1964**, *4* (5), 89–90.
- (16) Cui, Y.; Lauhon, L. J.; Gudiksen, M. S.; Wang, J. F.; Lieber, C. M. *Appl. Phys. Lett.* **2001**, *78* (15), 2214–2216.
- (17) Both the p-type and the n-type SiNWs were synthesized by chemical vapor deposition with 20 nm gold catalysts in a quartz tube furnace. For the p-type SiNWs, the feeding ratio of Si:B was 4000:1, and the growth condition was 440°C, 40 Torr, 10 sccm of Ar, 2.5 sccm of SiH<sub>4</sub>, and 3 sccm of 10000:1 H<sub>2</sub> diluted B<sub>2</sub>H<sub>6</sub>. For the n-type SiNWs, the feeding ratio of Si:P was 2000:1, 450°C, 40 Torr, 10 sccm of Ar, 2.5 sccm of SiH<sub>4</sub>, and 1.25 sccm of 1000:1 H<sub>2</sub> diluted PH<sub>3</sub>. The growth time was 15 min.
- (18) Devices were fabricated on degenerately doped silicon wafers with 500 nm thermally grown oxides. SiNWs suspended in an ethanol solution were deposited onto the silicon substrate, and the source and drain electrodes were defined by photolithography, metallization of Ti/Pd (2 nm/50 nm) by an electron beam evaporator, and lift-off. The devices were further passivated by 2 μm of SU-8 (Microchem Corp.) with a second photolithography step.
- (19) Kirby, B. J.; Hasselbrink, E. F. *Electrophoresis* **2004**, *25* (2), 187–202.
- (20) van der Heyden, F. H. J.; Stein, D.; Dekker, C. *Phys. Rev. Lett.* **2005**, *95* (11), 116104.
- (21) Mansouri, A.; Scheuerman, C.; Bhattacharjee, S.; Kwok, D. Y.; Kostiuik, L. W. *J. Colloid Interface Sci.* **2005**, *292* (2), 567–580.
- (22) Vanwagenen, R. A.; Andrade, J. D. *J. Colloid Interface Sci.* **1980**, *76* (2), 305–314.
- (23) Chun, M. S.; Lee, T. S.; Choi, N. W. *J. Micromech. Microeng.* **2005**, *15* (4), 710–719.
- (24) Burgreen, D.; Nakache, F. R. *J. Phys. Chem.* **1964**, *68* (5), 1084–1091.
- (25) Bournon, B.; Wong, J.; Miko, C.; Forro, L.; Bockrath, M. *Nat. Nanotechnol.* **2007**, *2* (2), 104–107.
- (26) Probst, R. F. *Physicochemical Hydrodynamics*, 2nd ed.; Wiley Interscience: New York, 2003.
- (27)  $\sigma = \sum_{i=1}^N F z_i^2 \mu_i C_i$  (S m<sup>-1</sup>), where the summation is over all the ionic species,  $F$  is Faraday's constant (c mol<sup>-1</sup>),  $z_i$  is the valency of each ionic species,  $\mu_i$  is the mobility of the ionic species (mol s kg<sup>-1</sup>), and  $C_i$  is the ionic concentration (mol m<sup>-3</sup>).
- (28) Cheng, Y.; Yun, C. S.; Strouse, G. F.; Zheng, J. P.; Yang, R. S.; Wang, Z. L. *Nano Lett.* **2008**, *8* (12), 4179–4184.
- (29) Ethanol (CH<sub>3</sub>CH<sub>2</sub>OH) is an amphiprotic solvent that can accept and donate protons through autoprotolysis reaction [2CH<sub>3</sub>CH<sub>2</sub>OH(aq) ↔ CH<sub>3</sub>CH<sub>2</sub>O<sup>-</sup>(aq) + CH<sub>3</sub>CH<sub>2</sub>OH<sub>2</sub><sup>+</sup>(aq)] (see refs 30 and 31). Amphiprotic solvents can also accept or donate protons if the system contains other proton donors/acceptors, such as the silica surface (Si-OH) or impurities like water (see refs 32 and 33). The existence of ions in ethanol is supported by the fact that the zeta potential of silica surface in ethanol was measured to be -72.6 mV (see ref 34). Moreover, streaming potential has been measured in ethanol and the reported streaming potential in ethanol was 2.4 times higher than that in water (see ref 35).
- (30) Letcher, T. M., *Developments and Applications in Solubility*; Royal Society of Chemistry: London, 2007.
- (31) Kim, D.; Posner, J. D.; Santiago, J. G. *Sens. Actuators, A* **2008**, *141* (1), 201–212.
- (32) Sharp, K. G. *J. Sol-Gel Sci. Technol.* **1994**, *2*, 35–41.
- (33) Kilic, E.; Aslan, N. *Microchim. Acta* **2005**, *151*, 89–92.
- (34) Valko, I. E.; Siren, H.; Riekkola, M. L. *J. Microcolumn Sep.* **1999**, *11* (3), 199–208.
- (35) Caldwell, K. D.; Myers, M. N. *Anal. Chem.* **1986**, *58* (7), 1583–1585.

NL900238A